

# RSC Advances



This is an *Accepted Manuscript*, which has been through the Royal Society of Chemistry peer review process and has been accepted for publication.

*Accepted Manuscripts* are published online shortly after acceptance, before technical editing, formatting and proof reading. Using this free service, authors can make their results available to the community, in citable form, before we publish the edited article. This *Accepted Manuscript* will be replaced by the edited, formatted and paginated article as soon as this is available.

You can find more information about *Accepted Manuscripts* in the [Information for Authors](#).

Please note that technical editing may introduce minor changes to the text and/or graphics, which may alter content. The journal's standard [Terms & Conditions](#) and the [Ethical guidelines](#) still apply. In no event shall the Royal Society of Chemistry be held responsible for any errors or omissions in this *Accepted Manuscript* or any consequences arising from the use of any information it contains.

## ARTICLE

## Enhanced carrier localization in near-ultraviolet multiple quantum wells by using quaternary AlInGaN as well layers

Cite this: DOI: 10.1039/x0xx00000x

Tong Liu,<sup>a</sup> Shujie Jiao,<sup>\*ab</sup> Hongwei Liang,<sup>c</sup> Tianpeng Yang,<sup>d</sup> Dongbo Wang<sup>a</sup> and Liancheng Zhao<sup>a</sup>Received 00th January 2012,  
Accepted 00th January 2012

DOI: 10.1039/x0xx00000x

[www.rsc.org/](http://www.rsc.org/)

The structural and optical properties of near-ultraviolet (UV) multiple quantum wells (MQWs) structure by using quaternary AlInGaN as well layers has been investigated. The composition of barrier layers is determined by three  $\text{In}_{0.08}\text{Ga}_{0.92}\text{N}/\text{Al}_x\text{In}_y\text{Ga}_{1-x-y}\text{N}$  multiple quantum wells samples with varying Al content in barrier layers. The composition of the well and barrier layers is estimated by the results of high-resolution X-ray diffraction (HRXRD). In spite of the larger lattice mismatch, the remarkable enhancement of photoluminescence (PL) intensity of the MQWs sample with AlInGaN as well layers is attributed to the increase of the carrier localized states induced by the increase of the compositional fluctuation in the AlInGaN well layers. The S-shaped temperature-dependence of PL peak energy indicates the existence of localized states induced by the potential fluctuations. The magnitude of carrier localization which is estimated by the fitting results has been increased significantly in the  $\text{Al}_{0.11}\text{In}_{0.13}\text{Ga}_{0.76}\text{N}/\text{Al}_{0.16}\text{In}_{0.045}\text{Ga}_{0.795}\text{N}$  MQWs due to the improvement of the spatial potential fluctuations by using quaternary AlInGaN as well layers.

### Introduction

III-nitride-based ultraviolet multiple quantum wells light emitting diodes (LEDs) and laser diodes (LDs) have attracted great attention in recent years for the extensive potential applications in photocatalyst<sup>1</sup> and high-density optical storage systems,<sup>2</sup> especially in solid-state lighting by using near-UV LEDs light owing to the high conversion efficiency of phosphors.<sup>3</sup> The high-efficiency LEDs devices can be achieved by the existence of localized exciton states in the active regions.<sup>4</sup> In conventional LEDs, InGaN/GaN MQWs structures have been used as active region for the green, blue and near-UV emission and lead to successful commercialization nowadays. Due to the formation of potential minima at the In-segregation regions in InGaN well layers, the carrier capture is more efficient than the nonradiative recombination centers.<sup>5</sup> However, the internal quantum efficiency is still limited by the weaker carrier confinement effect in the InGaN/GaN near-UV LEDs because of the small band offset in the quantum wells (QWs). In order to obtain larger carrier confinement, the AlGaIn is also used as barrier layers which have larger band offsets in the QWs. Nevertheless, the existence of biaxial strain and poor material quality extremely limit the use of the InGaN/AlGaIn MQWs.<sup>6</sup>

Recently, it has been suggested that the optical properties and carrier confinement were enhanced when quaternary AlInGaN was used in place of GaN barrier layers in near-UV LEDs,<sup>7</sup> due

to the lattice constant and band gap of the quaternary AlInGaN can be independently controlled by adjusting the composition of AlN, InN and GaN.<sup>8-11</sup> We have reported that the carrier localization can be improved by optimizing the Al composition of barrier layers in the blue  $\text{In}_{0.20}\text{Ga}_{0.80}\text{N}/\text{AlInGaN}$  MQWs with emission wavelength around 450 nm.<sup>9</sup>

In recent years, several research groups reported the AlInGaN/AlInGaN near-UV MQWs LEDs with greater carrier localization<sup>12,13</sup> due to the uniform growth condition and small lattice mismatch between well and barrier layers. Mee-Yi Ryu *et al.* suggested that the PL properties dominated by localized carriers in the AlInGaN MQWs agree well with those of the InGaN/GaN MQWs with a high density of localized states.<sup>14,15</sup> P. Lefebvre *et al.* reported that the in-plane localization of carriers induced by local potential fluctuations can be enhanced by the optimum well width.<sup>16</sup> However, the mechanism of the great carrier localization in the quaternary well layers is not clear yet. In this work, we study the carrier localization effect of the  $\text{Al}_x\text{In}_y\text{Ga}_{1-x-y}\text{N}/\text{Al}_x\text{In}_y\text{Ga}_{1-x-y}\text{N}$  MQWs structures. Due to the carrier localization can also be influenced by the composition of barrier layers. Thus, three  $\text{In}_{0.08}\text{Ga}_{0.92}\text{N}/\text{Al}_x\text{In}_y\text{Ga}_{1-x-y}\text{N}$  MQWs samples were first grown with the similar emission energy to optimize the barrier composition.

### Experimental

All samples were grown on *c*-plane sapphire substrates by a Thomas Swan 19×2" metalorganic chemical vapor deposition (MOCVD) system. Trimethylaluminum (TMAI), trimethylindium (TMIn), triethylgallium (TEGa) and ammonia (NH<sub>3</sub>) were used as the source precursors for Al, In, Ga and N, respectively. The sapphire substrate was first heated to 1100 °C in hydrogen ambient for the thermal cleaning treatment. Then, a 25-nm-thick low temperature GaN buffer layer was grown followed by a 1.5-μm-thick undoped GaN template layer. Afterwards, a ten-period MQWs structure was deposited with 2.5-nm-thick In<sub>0.08</sub>Ga<sub>0.92</sub>N well layers and 15-nm-thick Al<sub>*x*</sub>In<sub>*y*</sub>Ga<sub>1-*x-y*</sub>N barrier layers. During the growth process of barrier layers, the flow rates of TEGa, TMIn and NH<sub>3</sub> were maintained at constant and the flow rate of TMAI was set to be 3.5, 4.7 and 5.7 sccm, labeled as samples 1, 2 and 3, respectively. Besides, a MQWs structure with Al<sub>*x*</sub>In<sub>*y*</sub>Ga<sub>1-*x-y*</sub>N well layers was fabricated using the same barrier composition as sample 2 and labeled as sample 4. The detailed growth conditions have been published elsewhere.<sup>8-10</sup>

High-resolution X-ray diffraction was employed to analyze the structural parameters. Raman measurements were carried out to verify the existence of In-rich clusters. Temperature-dependent photoluminescence spectra were measured to investigate the carrier localization by using an iHR320 spectrometer with a He-Cd laser of 325 nm as the exciting source.

## Results and discussion

In order to obtain optimized alloy composition in well and barrier layers, three near-UV In<sub>0.08</sub>Ga<sub>0.92</sub>N/Al<sub>*x*</sub>In<sub>*y*</sub>Ga<sub>1-*x-y*</sub>N MQWs samples have been prepared. Fig. 1 shows the HRXRD (0002)  $\omega$ -2 $\theta$  scans of the MQWs samples. In order to determine the composition of Al<sub>*x*</sub>In<sub>*y*</sub>Ga<sub>1-*x-y*</sub>N barrier layers, some AlInGaN epilayers and similar MQWs structures were fabricated at the same growth conditions.<sup>9,10</sup> The detailed growth and structural parameters of the samples are listed in Table 1. The satellite peaks can be observed up to the fourth order, indicating the better interface quality and periodicity in the QWs. In the In<sub>0.08</sub>Ga<sub>0.92</sub>N/Al<sub>*x*</sub>In<sub>*y*</sub>Ga<sub>1-*x-y*</sub>N MQWs samples, the Al content of barrier layers increases with increasing TMAI flow rate. The smooth satellite peaks of sample 2 imply better lattice-match between barrier and GaN template layer. Then, sample 4 was grown with the same composition of the barrier layer as sample 2. Meanwhile, the composition of AlInGaN well layer was chosen to have the theoretically similar emission energy which is calculated by the following equations:<sup>17</sup>

$$E_g(\text{Al}_x\text{In}_y\text{Ga}_z\text{N}) = \frac{xyE_g^u(\text{AlInN}) + yzE_g^v(\text{InGaN}) + xzE_g^w(\text{AlGaN})}{xy + yz + zx} \quad (1)$$

$$E_g^u(\text{Al}_u\text{In}_{1-u}\text{N}) = uE_g(\text{AlN}) + (1-u)E_g(\text{InN}) - u(1-u)b(\text{AlInN}) \quad (2)$$

$$E_g^v(\text{In}_v\text{Ga}_{1-v}\text{N}) = vE_g(\text{InN}) + (1-v)E_g(\text{GaN}) - v(1-v)b(\text{InGaN}) \quad (3)$$

$$E_g^w(\text{Al}_w\text{Ga}_{1-w}\text{N}) = wE_g(\text{AlN}) + (1-w)E_g(\text{GaN}) - w(1-w)b(\text{AlGaN}) \quad (4)$$

where

$$u = (1-x+y)/2, \quad v = (1-y+z)/2, \quad w = (1-x+z)/2 \quad (5)$$

where *x*, *y* and *z* = 1 - *x* - *y* represent the content of Al, In and Ga in the quaternary Al<sub>*x*</sub>In<sub>*y*</sub>Ga<sub>1-*x-y*</sub>N, respectively. The *b*(AlInN), *b*(InGaN) and *b*(AlGaN) is the bandgap bowing parameter of the AlInN, InGaN and AlGaN, respectively.

The lattice mismatch *f* between well and barrier layers have been numerically evaluated to be 0.65%, 0.78%, 0.84% and 1% for the MQWs samples 1-4, respectively, by using the following expression:<sup>18</sup>

$$f = (a_w - a_b) / a_b \quad (6)$$

where *a<sub>w</sub>* and *a<sub>b</sub>* denote the lattice constants of well and barrier materials, respectively.

It has been confirmed that In-segregation effect taking place in the well layers of InGaN-based blue LEDs are the source of the high radiative recombination efficiency.<sup>19,20</sup> Raman scattering measurements have been carried out at room temperature to study the In-rich clusters in these near-UV MQWs samples. The inset of Fig. 2 shows the Raman scattering of sample 4 over the measurement range of 100–1000 cm<sup>-1</sup>. The scale was enlarged to get a clear picture for the Raman vibration of the In-rich clusters, as shown in Fig. 2. Two vibration modes, which can be clearly seen in these four samples at around 432 cm<sup>-1</sup> and 453 cm<sup>-1</sup>, were considered to be from the vibration of InN,<sup>9</sup> indicating the existence of nearly pure InN regions in the quantum wells. Therefore, the local potential fluctuations could be formed around the In-rich regions. Obviously, the intensities of the two vibration modes from sample 4 become stronger induced by the higher In content in the well layers. Moreover, the shift to lower frequency of the vibration peak positions in sample 4 is considered to be also affected by the increase of In content.<sup>21</sup>

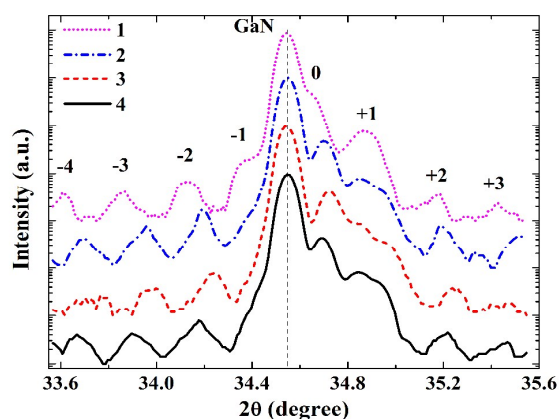


Fig. 1 HRXRD (0002)  $\omega$ -2 $\theta$  scans of the MQWs samples. Samples 1–3 are the MQWs with In<sub>0.08</sub>Ga<sub>0.92</sub>N well layers and sample 4 is the MQWs with Al<sub>0.11</sub>In<sub>0.13</sub>Ga<sub>0.76</sub>N well layers.

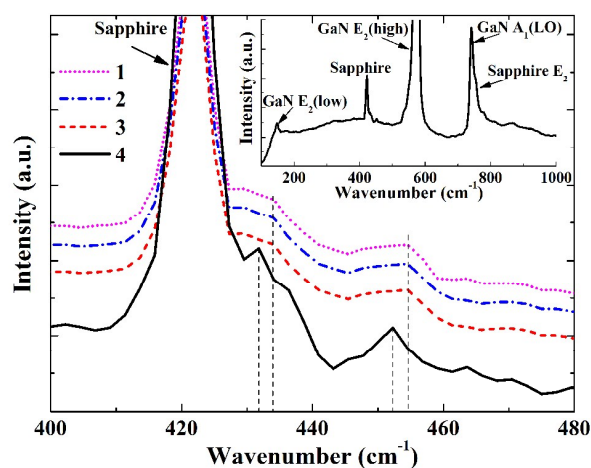


Fig. 2 Raman scattering of the MQWs samples at room temperature. The vertical dashed lines indicate the positions of the In-cluster related Raman vibrations. The inset is the Raman scattering of sample 4 over the measurement range of 100–1000 cm<sup>-1</sup>.

## ARTICLE

TABLE 1 Structural parameters and optical properties of the MQWs samples.

Sample	XRD				PL			
	Well		Barrier		10 K		300 K	
	Al (%)	In (%)	Al (%)	In (%)	Energy (eV)	FWHM (meV)	Energy (eV)	FWHM (meV)
1	0	8	15	5.5	3.194	52	3.173	123
2	0	8	16	4.5	3.232	52	3.198	123
3	0	8	17	4	3.199	54	3.169	126
4	11	13	16	4.5	3.171	61	3.150	134

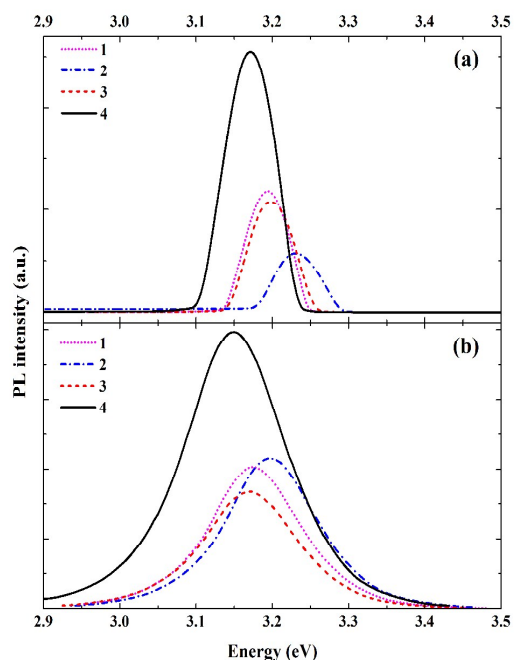


Fig. 3 PL spectra of the MQWs samples measured at (a) 10 K and (b) 300 K, respectively.

The PL spectra measurements of the MQWs samples were performed as depicted in Fig. 3(a) for 10 K and Fig. 3(b) for 300 K, respectively. At 10 K and 300 K, the PL spectra of the MQWs samples are dominated by a sharp emission peak. In the blue  $\text{In}_{0.20}\text{Ga}_{0.80}\text{N}/\text{Al}_x\text{In}_y\text{Ga}_{1-x-y}\text{N}$  MQWs, the PL emission peak energy exhibits clearly redshift with increasing Al content in barrier layers due to the increase of quantum-confined Stark effect (QCSE).<sup>9</sup> In this work, however, the PL emission peak energies of samples 1–3 with increasing Al content in barrier layers do not present this redshift. We speculate that the reduced band offsets in the QWs may be responsible for this phenomenon due to the larger bandgap of  $\text{In}_{0.08}\text{Ga}_{0.92}\text{N}$  well layers compared to that of blue MQWs. It is worth to note that the PL intensity of sample 4 is nearly twice as strong as that of the samples with  $\text{In}_{0.08}\text{Ga}_{0.92}\text{N}$  well layers in spite of the larger lattice mismatch up to 1% in the QWs. Moreover, the FWHM of the PL curve from sample 4 is larger than that of the other samples at either 10 or 300 K, as shown in Table 1. Therefore, we speculate that the intense emission

of sample 4 is attributed to the increase of the local compositional variation by introducing Al atoms into InGaN well layers, leading to the enhancement of the spatial potential fluctuation and carrier localization effect, and thus, the radiative recombination efficiency has been improved significantly.

The temperature-dependent PL spectra have been measured in the temperature range from 10 to 300 K to support our speculation that the carrier localization effect is enhanced by increasing the compositional fluctuation. The S-shaped temperature-dependence of PL peak energy in these MQWs samples, that is, redshift–blueshift–redshift, can be clearly observed in Fig. 4. This behavior is a well-known manifestation of the existence of the localized carriers in the

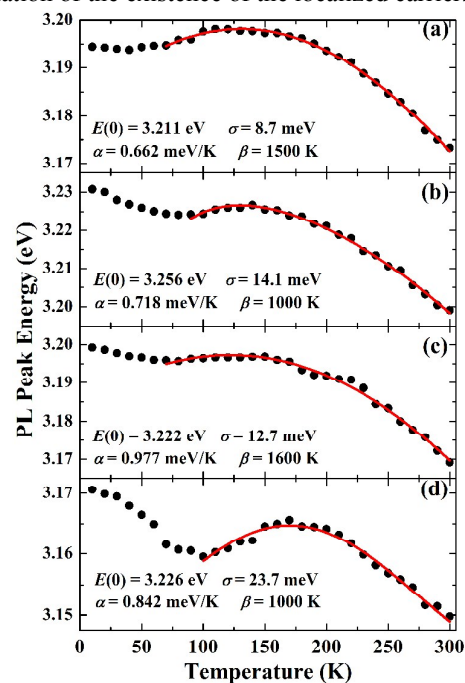


Fig. 4 PL emission peak energy as a function of temperature in the samples with MQWs of (a)  $\text{In}_{0.08}\text{Ga}_{0.92}\text{N}/\text{Al}_{0.15}\text{In}_{0.055}\text{Ga}_{0.795}\text{N}$ , (b)  $\text{In}_{0.08}\text{Ga}_{0.92}\text{N}/\text{Al}_{0.16}\text{In}_{0.045}\text{Ga}_{0.795}\text{N}$ , (c)  $\text{In}_{0.08}\text{Ga}_{0.92}\text{N}/\text{Al}_{0.17}\text{In}_{0.04}\text{Ga}_{0.79}\text{N}$  and (d)  $\text{Al}_{0.11}\text{In}_{0.13}\text{Ga}_{0.76}\text{N}/\text{Al}_{0.16}\text{In}_{0.045}\text{Ga}_{0.795}\text{N}$ . The solid dots stand for the measurement data. The solid line show the best fitting results with the Varshni empirical equation and the fitting parameters are also given in the figures.

QWs.<sup>22,23</sup> To estimate the magnitude of the carrier localization effect in these MQWs samples, the measurement results of the emission energy are fitted by the modified Varshni empirical equation:<sup>24</sup>

$$E(T) = E(0) - \alpha T^2 / (T + \beta) - \sigma^2 / K_B T \quad (7)$$

This equation is only valid for the temperature above 70 K.  $E(0)$  is the bandgap energy at 0 K;  $\alpha$  and  $\beta$  are Varshni thermal coefficients;  $K_B$  is the Boltzmann constant;  $\sigma$  indicates the magnitude of the localization effect, namely, larger value of  $\sigma$  means stronger carrier localization effect. The fitting results are plotted by the solid lines and the fitting parameters are also given in the Fig. 4 (a)–(d). The magnitude of the carrier localization increases dramatically in sample 4 compare with the  $\text{In}_{0.08}\text{Ga}_{0.92}\text{N}/\text{Al}_x\text{In}_y\text{Ga}_{1-x-y}\text{N}$  MQWs samples, indicating that more carriers are confined in the localized states in the QWs. Therefore, the radiative recombination efficiency will be improved significantly by introducing Al atoms into InGaN well layers due to the increase of the local potential fluctuation.

Alternatively, the transition temperature from redshift to blueshift of the MQWs samples 1–4 is 40, 80, 80 and 100 K, and that from blueshift to redshift is 110, 140, 150 and 170 K, respectively. The blueshift energy between the two transition temperatures is about 4, 3, 1 and 6 meV for these four MQWs samples, respectively. The expected temperature-reduced bandgap shrinkage (redshift) is about 5, 9, 11 and 13 meV for the corresponding temperature regions which is estimated from GaN.<sup>25</sup> Therefore, the actual blueshift energy of the emission peaks with respect to the band edge is about 9, 12, 12 and 19 meV, respectively. The larger amount of the blueshift energy means stronger carrier localization, which is in well accordance with the variation tendency of the magnitude of the localization effect ( $\sigma$ ).

## Conclusions

In summary, near-UV MQWs structure by using quaternary AlInGaN as well layers has been grown. In spite of the larger lattice mismatch, the PL intensity could be remarkably enhanced by substituting quaternary  $\text{Al}_{0.11}\text{In}_{0.13}\text{Ga}_{0.76}\text{N}$  for  $\text{In}_{0.08}\text{Ga}_{0.92}\text{N}$  well layers. It can be attributed to the increase of the carrier localized states induced by the increase of the local compositional variation. The S-shaped temperature-dependence of PL peak energy indicated that the magnitude of carrier localization effect which is estimated by the fitting results has been enhanced significantly by introducing Al atoms into InGaN well layers due to the improvement of the spatial potential fluctuations. Therefore, the carrier localization becomes strong enough to prevent their capture by the nonradiative recombination centers and the optical properties can be enhanced by using quaternary AlInGaN as well layers in the near-UV MQWs, which may open an opportunity for the GaN-based high-efficiency LEDs devices.

## Acknowledgements

This work was supported by National Science Foundation (No. 61306014); Harbin Special Fund for Creative Talents in Science and Technology (No. 2012RFLXG029); Research Fund for the Doctoral Program of Higher Education of China (No. 20122302120009); Open Project Program of Key Laboratory for Photonic and Electric Bandgap Materials, Ministry of Education, Harbin Normal University (No. PEBM201302).

## Notes and references

<sup>a</sup> School of Materials Science and Engineering, Harbin Institute of Technology, Harbin 150001, China. E-mail: [shujiejiao@gmail.com](mailto:shujiejiao@gmail.com); Tel: +86 451 86417763

<sup>b</sup> Key Laboratory for Photonic and Electric Bandgap Materials, Ministry of Education, Harbin Normal University, Harbin 150001, China

<sup>c</sup> School of Physics and Optoelectronic Engineering, Dalian University of Technology, Dalian 116024, China

<sup>d</sup> EpiTop Optoelectronic Co., Ltd., Pingxiang 337000, China

- P. M. Tu, C. Y. Chang, S. C. Huang, C. H. Chiu, J. R. Chang, W. T. Chang, D. S. Wu, H. W. Zan, C. C. Lin, H. C. Kuo and C. P. Hsu, *Appl. Phys. Lett.*, 2011, **98**, 211107.
- S. N. Lee, S. Y. Cho, H. Y. Ryu, J. K. Son, H. S. Paek, T. Sakong, T. Jang, K. K. Choi, K. H. Ha, M. H. Yang, O. H. Nam, Y. Park and E. Yoon, *Appl. Phys. Lett.*, 2006, **88**, 111101.
- M. Shatalov, A. Chitmis, V. Adivarahan, A. Lunev, J. Zhang, J. W. Yang, Q. Fareed, G. Simin, A. Zakheim, M. Asif Khan, R. Gaska and M. S. Shur, *Appl. Phys. Lett.*, 2001, **78**, 817.
- H. Zhu, C. X. Shan, B. H. Li, Z. Z. Zhang, J. Y. Zhang, B. Yao, D. Z. Shen and X. W. Fan, *J. Appl. Phys.*, 2009, **105**, 103508.
- J. Zhang, J. Yang, G. Simin, M. Shatalov, M. Asif Khan, M. S. Shur and R. Gaska, *Appl. Phys. Lett.*, 2000, **77**, 2668.
- D. Zhu, M. J. Kappers, P. M. F. J. Costa, C. McAleese, F. D. G. Rayment, G. R. Chabrol, D. M. Graham, P. Dawson, E. J. Thrush, J. T. Mullins and C. J. Humphreys, *Phys. Status Solidi A*, 2006, **203**, 1819.
- S. H. Baek, J. O. Kim, M. K. Kwon, I. K. Park, S. I. Na, J. Y. Kim, B. Kim and S. J. Park, *IEEE Photonics Technol. Lett.*, 2006, **18**, 1276.
- T. Liu, S. J. Jiao, D. B. Wang, L. C. Zhao, T. P. Yang and Z. G. Xiao, *Appl. Surf. Sci.*, 2014, **301**, 178.
- T. Liu, S. J. Jiao, D. B. Wang, S. Y. Gao, T. P. Yang, H. W. Liang and L. C. Zhao, *J. Alloys Compd.*, 2015, **621**, 12.
- D. B. Wang, S. J. Jiao, L. C. Zhao, T. Liu, S. Y. Gao, H. T. Li, J. Z. Wang, Q. J. Yu and F. Y. Guo, *J. Phys. Chem. C*, 2013, **117**, 543.
- S. Suihkonen, O. Svensk, P. T. Törmä, M. Ali, M. Sopanen, H. Lipsanen, M. A. Odnoblyudo and V. E. Bougrov, *J. Cryst. Growth*, 2008, **310**, 1777.
- T. Wang, G. Raviprakash, F. Ranalli, C. N. Harrison, J. Bai, J. P. R. David, P. J. Parbrook, J. P. Ao and Y. Ohno, *J. Appl. Phys.*, 2005, **97**, 083104.
- Y. Liu, T. Egawa, H. Ishikawa, H. Jiang, B. Zhang, M. Hao and T. Jimbo, *J. Cryst. Growth*, 2004, **264**, 159.
- M. Y. Ryu, C. Q. Chen, E. Kuokstis, J. W. Yang, G. Simin and M. Asif Khan, *Appl. Phys. Lett.*, 2002, **80**, 3730.
- M. Y. Ryu, C. Q. Chen, E. Kuokstis, J. W. Yang, G. Simin, M. Asif Khan, G. G. Sim and P. W. Yu, *Appl. Phys. Lett.*, 2002, **80**, 3943.
- P. Lefebvre, S. Anceau, P. Valvin, T. Taliercio, L. Konczewicz, T. Suski, S. P. Lepkowski, H. Teisseyre, H. Hirayama and Y. Aoyagi, *Phys. Rev. B*, 2002, **66**, 195330.
- A. J. Ghazai, S. M. Thahab, H. Abu Hassan and Z. Hassan, *Optik*, 2012, **123**, 856.

## Journal Name

- 18 A. Shalimov, J. Bąk-Misiuk, V. M. Kaganer, M. Calamiotou and A. Georgakilas, *J. Appl. Phys.*, 2007, **101**, 013517.
- 19 Y. J. Sun, O. Brandt, B. Jenichen and K. H. Ploog, *Appl. Phys. Lett.*, 2003, **83**, 5178.
- 20 S. Y. Karpov, R. A. Talalaev, I. Y. Evstratov and Y. N. Makarov, *Phys. Status Solidi A*, 2002, **192**, 417.
- 21 M. R. Correia, S. Pereira, E. Pereira, J. Frandon and E. Alves, *Appl. Phys. Lett.*, 2003, **83**, 4761.
- 22 X. A. Cao, S. F. LeBoeuf, L. B. Rowland, C. H. Yan and H. Liu, *Appl. Phys. Lett.*, 2003, **82**, 3614.
- 23 Y. H. Cho, G. H. Gainer, A. J. Fischer, J. J. Song, S. Keller, U. K. Mishra and S. P. DenBaars, *Appl. Phys. Lett.*, 1998, **73**, 1370.
- 24 P. G. Eliseev, P. Perlin, J. Lee and M. Osiński, *Appl. Phys. Lett.*, 1997, **71**, 569.
- 25 B. Monemar, *Phys. Rev. B*, 1974, **10**, 676.